The flexural strength of bonded ice

Andrii Murdza[1], Arttu Polojärvi[2], Erland M. Schulson[1], Carl E. Renshaw[1,3]

[1]Thayer School of Engineering, Dartmouth College, Hanover, NH, USA

[2]Aalto University, School of Engineering, Department of Mechanical Engineering, P.O. Box 14100, 00076 Aalto, Finland

[3]Department of Earth Sciences, Dartmouth College, Hanover, NH, USA

Correspondence to: Andrii Murdza (Andrii.Murdza@dartmouth.edu)

Abstract. The flexural strength of ice surfaces bonded by freezing, termed freeze-bond, was studied by performing four-point-bending tests of bonded freshwater S2 columnar-grained ice samples in the laboratory. The samples were prepared by milling the surfaces of two ice pieces, wetting two of the surfaces with water of varying salinity, bringing these surfaces together, and then letting them freeze under a compressive stress of about 4 kPa. The salinity of the water used for wetting the surfaces to generate the bond varied from 0 to 35 ppt. Freezing occurred in air under temperatures varying from -25 to -3 °C over periods that varied from 0.5 h to ~100 hours. Results show that an increase in bond salinity or temperature leads to a decrease in bond strength. The trend for the bond strength as a function of salinity is similar to that presented in Timco and O'Brien (1994) for saline ice. No freezing occurs at -3 °C once the salinity of the water used to generate the bond exceeds ~25 ppt. The strength of the saline ice bonds levels off (i.e., saturates) within 6-12 hours of freezing; bonds formed from fresh water reach strengths that are comparable or higher than that of the parent material in less than 0.5 hours.

1. Introduction

Freeze bonds form when distinct ice features, such as floating ice floes or ice blocks of a rubble pile, become and remain in contact over a period of time at low enough temperature. Insight into the strength of the bonds is important when, for example, the strength of an ice cover formed of refrozen floes or the strength of an ice rubble pile is estimated. There are several factors that affect the failure of a cover of sea ice, surface waves being a major one that has gained an increasing amount of interest recently (Shen, 2017; Squire, 2020). Under the action of waves, ice covers bend and may undergo flexural failure (Ardhuin et al., 2020; Asplin et al., 2012; Collins et al., 2015; Hwang et al., 2017; Kohout et al., 2014, 2016; Shackleton, 1982). It is relevant to ask if the freeze bonds forming into vertical cracks within a broken and refrozen ice cover form the weakest link at which wave-induced cracks initiate and propagate. During the wave-ice interaction, the freeze bonds deform and failure occurs under a tensile state of stress arising from flexural deformation. Szabo and Schneebeli (2007) performed tensile tests on sintered ice grains on scale ~10^{-3} m, but to our knowledge, no data on freeze-bond strength under tensile loading at time and length scales relevant to geophysical or ice engineering problems have been published.

33   The strength of freeze bonds has been tested only under combined compressive and shear loading. Such tests
34   have been related to continuum modeling of ice rubble using material models having yield surfaces resembling that
35   of a Mohr-Coulomb material model (Ettema and Urroz, 1989; Heinonen, 2004; Liferov et al., 2002, 2003; Serré,
36   2011b, 2011a). The critical shear stress of a Mohr-Coulomb material is given by $\tau = c + \sigma \tan \varphi$, where c is the
37   cohesion, σ the compressive stress, and φ the internal friction angle of the material. The underlying assumption in
38   testing has been that the failure of the individual freeze bonds within the rubble occurs through the same mode as the
39   failure of the rubble itself. No evidence of this type of similarity between the two scales exists. Instead, the numerical
40   simulations (Polojärvi and Tuhkuri, 2013) suggest that the individual freeze bonds within deforming rubble do not
41   fail due to shear, but rather under tensile stresses as the bonded ice blocks move relative to each other. This implies
42   that data on the shear strength of the freeze bonds may not lead to reliable estimates of the shear strength of ice rubble.
43
44   In this paper, the strength of freeze bonds under tensile loading is studied. For this purpose, we conducted
45   four-point-bending tests using the apparatus described and used by Murzda et al. (2020). All procedures for testing
46   were designed with the aim of reducing the number of variables for reliable analysis: bonds were formed between
47   milled surfaces of freshwater ice specimens (termed the parent material) and bond freezing and testing were performed
48   in air under a small compressive stress of about 4 kPa. The experimental variables were the freezing time (0.5 h…~100
49   h), the sample temperature (-3°C…-25°C), and the salinity of the water used to form the bond (0…35 ppt). Bond
50   strength initially increases with freezing time, but then appears to level off and to reach a plateau (i.e., to saturate)
51   over several hours. Depending on the salinity of the water from which the bond is formed, the saturation time for bond
52   strength ranges from 0.5 h to 12 h. The "saturated strength" of freshwater bonds with finer microstructure appears to
53   reach levels higher than the strength of the parent material with a larger grain size. The results from these experiments,
54   presented below, represent the first set of results on the failure of freeze bonds under tension.

55   **2. Experimental procedure**

56   Freshwater ice, used here as the parent material for the freeze-bonded samples, was produced in the
57   laboratory as described in Smith and Schulson (1993) and Golding and others (2010). Tap-water was frozen
58   unidirectionally from top to bottom in a cylindrical 800 L polycarbonate tank, forming pucks of ~1 m in diameter and
59   ~25 cm in thickness. The ice was generally bubble-free and columnar-grained. Thin-section analysis showed that the
60   average column diameter, as measured in the horizontal plane normal to the direction of ice growth using the linear
61   intercept method, was 5.5±1.3 mm. The c-axes were randomly oriented within, and confined to, the horizontal plane,
62   suggesting that the ice had an S2 growth texture (in the terminology of Michel and Ramseier, 1971). The ice density
63   was 914.1±1.6 kg·m^{-3} (Golding and others, 2010); Young's modulus in the horizontal plane was 9.52 GPa (Snyder
64   and others, 2016). Once grown, the ice was cut into blocks and stored in plastic cooler boxes in a cold room at -10º C.
65   Specimen preparation is described in detail elsewhere (Iliescu et al., 2017; Murzda et al., 2018, 2019, 2020c, 2020a).
66

67   Samples to be freeze-bonded were prepared from the ice blocks by milling them into thin plates. The plates

68   had dimensions of h ~15 mm in thickness (parallel to the long axis of the grains), b ~ 85 mm in width, and l ~300 mm

69   in length. Specimens were allowed to equilibrate to the test temperature for at least 24 hours prior to testing.

70

71   The plates were then cut perpendicular to their long axis into two parts. In most samples the sawn surfaces

72   were milled after cutting (more below). The two parts of the specimen were then placed in a cold room with a

73   temperature of +2°C for a few minutes. To initiate freeze-bond growth, the sawn and milled surfaces were sprayed

74   with a fine mist of water at a temperature of +2°C and quickly brought into contact by setting the two pieces into a

75   freeze-bonding rig (Figure 1). The surfaces were wet when brought into contact, but in addition, a syringe was used

76   to inject about 0.1 ml of water to the bond to ensure uniform wetting of the surfaces. Excess water, if any was observed

77   around the bond, was wiped with a tissue. All of the above steps were performed at +2 °C to prevent freezing from

78   occurring before setting the sample into the rig. Afterwards, the freeze-bonding rig was moved to another cold room

79   with a desired test temperature.

80

81   To investigate whether the roughness of the faces in contact affects the bond strength, a few samples had

82   their faces produced by cutting the parent plate either with a coarse (1/2 inch in width, 1/40 inch in thickness and

83   6 teeth per inch) or a fine (13/64 inch in width, 1/64 inch in thickness and 24 teeth per inch) band saw. Although few

84   in number, results from these initial experiments suggested that surface roughness of the kind we explored had no

85   significant effect on flexural strength. Thus, for all further tests (that led to the results reported below) sawn surfaces

86   were milled for consistency and reproducibility (more in Discussion).

87

88   Figure 1 shows a sketch (a) and photograph (b) of the freeze-bonding rig. The rig had a system consisting of

89   two plastic bars and two springs for applying a desired pressure (i.e., compressive stress) to the bond during freezing.

90   In the present experiments, a confining pressure of ~4 kPa was chosen which is in accordance with the maximum

91   hydrostatic pressure within submerged 10-meter-thick ice rubble mass (Ettema and Schaefer, 1986). The rig was kept

92   in a cold room of the desired temperature (i.e. from -25°C to -3°C) during freezing. The base of the rig was made from

93   an acrylic plate having low heat conductivity, ensuring the heat flux in the bond area was mainly along the long axis

94   of the sample. Wax paper was placed between the ice and the acrylic to prevent freezing of ice onto the rig. All

95   materials of the rig were such that the frictional resistance between them and ice was low. This enabled good control

96   of the confining pressure and sample alignment.

97

98   To investigate the effect of the salinity on the bond strength, fresh water and saline water of salinity ranging

99   from 2 to 35 ppt (parts per thousand), was used in spraying. Saline water was prepared in the manner described by

100   Golding et al. (2010, 2014) by adding the commercially available salt mixture "Instant Ocean" to tap water. Salinity

101   was measured using a calibrated YSI Pro30 conductivity salinity meter.

102

103   After a desired time of freezing, varying from 0.5 to ~100 h, the freeze-bonded sample was removed from
104   the rig and its flexural strength under four-point bending was measured. For this purpose, a servo-hydraulic loading
105   system (MTS model 810.14) with a custom-built four-point loading frame was utilized. The sketch of the apparatus
106   is shown in Figure 2 of Murdza et al. (2020c), the photograph of the apparatus is shown in Figure 5a and the apparatus
107   is described in detail elsewhere (Iliescu et al., 2017; Murdza et al., 2018, 2019, 2020c). The outer loading rollers are
108   immobile during testing while the inner loading rollers are attached to the actuator. The hydraulic actuator was driven
109   under displacement control and loading was controlled using a FlexTest-40 controller. A calibrated load cell was used
110   to measure the load.
111
112   The experiments were performed at an outer-fiber center-point displacement rate of 0.1 mm s^{-1} (or outer-
113   fiber strain rate of about 1.4 x 10^{-4} s^{-1} according to linear-elastic first order beam theory). This displacement rate
114   resulted in an outer-fiber stress rate of about 1 MPa s^{-1}. As was indicated earlier (Murdza et al., 2020c), the 0.1 mm s^{-1}
115   displacement rate in cycling results in a period of ~20 s which is approximately the frequency of ocean swells (Collins
116   and others, 2015). The major outer-fiber stress σ_f was calculated as:

$$\sigma_f = \frac{3PL}{4bh^2} \ ,$$ (1)

117   where P is the applied load and L is the distance between the outer pair of loading cylinders and is set by the geometry
118   of the apparatus to be $L = 254$ mm. The flexural strength that we refer to throughout this paper is the maximum major
119   outer-fiber stress that the ice plate can withstand before breaking (assuming the material is linear-elastic and brittle).
120   It is important to note that in all experiments described in this paper the bond formation and breaking of bonded ice
121   occurred at the same temperature. Owing to the confining impact of the loading cylinders of the 4-point flexing
122   apparatus (see Figure 5a and Figure 2 of Murdza et al. (2020c)) and to the Poisson effect, a biaxial state of tension
123   developed in the ice.

124   **3. Results and Observations**

125   **3.1. Flexural strength of parent material**

126   Two measurements on the flexural strength of pristine ice plates, that is, plate-like samples of parent material
127   without a freeze bond, were conducted at -10 °C. The strength values obtained were 1.51 and 1.63 MPa. Only two
128   experiments were performed as these values compare favorably with the earlier measurements (Murdza et al., 2020c)
129   on the same kind of ice using the same loading system. Murdza et al. (2020c) reported that the average and the standard
130   deviation of the flexural strength at -3, -10 and -25 °C were 1.42±0.16, 1.67±0.22 and 1.89±0.01 MPa, respectively.
131   Further, the measured values are in agreement with the data that are reviewed in Timco and O'Brien (1994), where
132   the average and standard deviation of 1.73±0.25 MPa is reported for the flexural strength of freshwater ice at
133   temperatures below -4.5 °C.

3.2. Flexural strength of bonded ice

3.2.1. Freshwater bond

The experiments with a freshwater bond were conducted at -3 and -10 °C. The results are listed in Table 1. The shortest time of 0.5 hours used here for the bond formation implies that the bond formed in less time. Surprisingly, in all of these experiments, the failure occurred outside of the bond. This suggests that even after only a relatively short period of freezing, the strength of the freshwater bond reaches and exceeds that of the parent material. Even though the results listed in Table 1 show scatter, at -10°C comparison of the measured flexural strengths to those described in Section 3.1 showed that they are not statistically different from the flexural strength of pristine freshwater ice samples (*p-value* = 0.21 and 0.08 for tests at -3 and -10 °C, respectively). This is important because it indicates that the above-described bond generation procedure did not hamper the samples by, for example, leading to geometrical misalignments in them.

3.2.2. Saline bond

Figures 2 and 3 show the results from the experiments performed to investigate the effect on bond strength of the salinity of the water used to create the freeze bond. The data are given in Tables 2-4. The tables indicate the experiments where no freezing occurred ("No") and the experiments where bonding occurred, but the bond was too weak to be tested ("Low"). These data are excluded in the figures below.

Figure 2 shows that the strength of the saline bonds increases over time and levels off, or saturates, after about 6-12 h. Thus, the strength of the saline bonds increases at a considerably lower rate than that of the freshwater bonds. A comparison of these results to those in Section 3.1 shows that the strength of the saline bonds is well below the strength of the freshwater ice used as the parent material. A comparison of the two data sets in Figure 2 shows that the saturated strength of the bonds made from water of higher salinity but at lower temperature (35 ppt and -10 °C) is about twice of that of the bonds with lower salinity but higher temperature (12 ppt and -3 °C).

Figure 3 illustrates how the salinity of the water used to generate the freeze-bond at -3 °C affects its saturated strength at -3 °C. While the measured strength values for low salinities are close to those measured for freshwater ice, the bond strength decreases rapidly with an increase in salinity and no freezing occurs once the salinity of the salt water used to generate the bond reaches ~25 ppt; even at 17 ppt some bonds were too weak to be tested. This agrees reasonably well with analytical estimates, Appendix A, where formulas that relate strength to volume fraction of solid phase suggest that at salinities of 30 ppt and above at -3 °C no freezing occurs. Figure 3 additionally shows two exponential fits, one directly fitted to our data and one by Timco and O'Brien (1994) for the flexural strength of saline ice (equations for these fits provided in Appendix B, where σ_b is flexural strength in MPa and ν_b is liquid brine content in parts per thousand). It is important to notice that the fit by Timco and O'Brien (1994) yields lower values than the measured bond strength in the present study for the whole range of salinities used. Likewise, the actual strength values for the freshwater bonds are greater than the ones suggested by Figure 3, since the failure in these cases occurred outside the bond, indicating that the bond is stronger than the parent material. Both saline and freshwater bonds that

169 develop through freezing appear to reach strengths higher than that of S2 type parent material of the same salinity

170 (strength of saline parent material is assumed to be the same as in Timco and O'Brien (1994)).

171   Temperature has a strong effect on the saturated strength of the freeze bonds. Figure 4 and Table 5 summarize

172 the data from experiments on specimens having bonds made from water of salinity 20 ppt at temperatures from -3 °C

173 to -25 °C. Three out of the four specimens at -25 °C failed outside of the bond with a measured strength of

174 1.61±0.12 MPa, which is close to 1.89 MPa measured earlier at -25 °C on the same type of freshwater ice (Murdza et

175 al., 2020c). Figure 4 also suggests that no freezing occurs at temperatures above about -3 °C, which is in fair agreement

176 with analytical estimates of no strength at T = -2 °C in Appendix A. Though the analytical equation from Appendix A

177 predicts well when no freezing occurs, it does not yield a trend that describes most of the data in Figure 4. The reason

178 may be that for the microstructure of bonds in the present study, strength may not be directly proportional to volume

179 fraction of the solid phase as the model in Appendix A assumes, but rather a non-linear function of the volume fraction

180 of solid.

181   Figure *5*a-c show an example of the typical samples after failure. Figure *5*a shows a case where the crack had

182 initiated at the bond and started to propagate along it, but then deviated from it and continued to grow through the

183 parent material. Figure 5b shows a close up of a bond face-on after the most common type of failure, which occurred

184 along the bond. In this case, both surfaces of the failed freeze-bond had a fairly uniform "blurry" appearance which

185 indicates that failure occurred through the ice of the bond. It was also fairly usual for the samples having low salinities,

186 low temperatures and long freezing times, that the crack initiated and started to propagate along the bond and then

187 slightly deviated and moved parallel to the bond but inside the parent material, as shown by Figure 5c.

188 **4. Discussion**

189   The above results are the first measurements to be reported for the strength of freeze bonds under tensile

190 loading. Although the experiments were performed under flexural loading, they provide unique data on the tensile

191 strength of the freeze bonds. Under the loading conditions, the flexural strength of ice is governed by tensile strength

192 (assuming the material is linear-elastic and brittle), although measured strengths are greater by a factor of about 1.7

193 than strengths measured under pure tensile loading (Ashby and Jones, 2012). The reason is that in bending only a thin

194 layer close to one surface of the sample (and thus a relatively small volume) carries the peak tensile stress and it is

195 less likely that this volume contains larger flaw, while in tension the entire sample carries the tensile stress and it is

196 more likely that it will contain larger flaws. Murdza et al. (2020b) showed that the flexural strength of freshwater S2

197 ice tested on the same loading system as used here compares well with direct measurements of the tensile strength of

198 the same type of ice at the same conditions (Carter, 1971) when divided by 1.7. Murdza et al. (2020b, 2021) showed

199 that the flexural strength of lake Arctic ice tested under three-point bending is also similar to the the one obtained in

200 Murdza et al. (2020b). By using this 1.7 factor to scale the values for saturated bond strengths shown in Figure 2 leads

201 to tensile strength values of about 0.3 MPa and 0.18 MPa for bonds at -10 °C and -3 °C, respectively.

202

203   While there are no other data on the tensile strength of freeze bonds, the results can be compared to the
204   relatively large amount of earlier work on the shear strength of freeze bonds (Bailey et al., 2012; Boroojerdi et al.,
205   2020a, 2020b; Bueide and Høyland, 2015; Ettema and Schaefer, 1986; Helgøy et al., 2013b, 2013a; Høyland and
206   Møllegaard, 2014; Marchenko and Chenot, 2009; Repetto-Llamazares et al., 2011b, 2011a; Serré et al., 2011; Shafrova
207   and Høyland, 2008; Szabo and Schneebeli, 2007). Common values for the shear strength in those studies ranged from
208   0.01 to 0.1 MPa, which are considerably lower than the flexural strength values measured here. Usually, these
209   strengths have been measured for bonds grown under water over periods that have not been long enough to reach
210   saturated bond strengths. On the other hand, the highest reported shear strength values ~0.3…0.7 MPa (Bailey et al.,
211   2012; Boroojerdi et al., 2020b; Shafrova and Høyland, 2008) are within the same range as the flexural strength values
212   measured here. Given that the tensile strength of ice is, on average, lower than the shear strength (Timco and Weeks,
213   2010), the strength values measured here are perhaps surprisingly high. The high strength values here likely relate to
214   the well-controlled bond growing procedure and possibly to a finer microstructure of the material that comprises the
215   bond.

216

217   Work on the shear strength of freeze bonds has led to a conclusion that the evolution of the bond strength has
218   three phases (Boroojerdi et al., 2020b; Repetto-Llamazares et al., 2011b, 2011a): (1) an initial period of a few minutes
219   of increasing strength due to heat flux from the bond to the parent material; (2) a period of some hours of weakening
220   as the temperature of the bond increases due to water surrounding it; and, (3) a period of several days of strengthening
221   due to sintering. The evolution of the flexural strength of the bonds in the present experiments is likely similar to that
222   of phases (1) and (3). The initial bond strengthening can be related to the transfer of heat along the long axis of the
223   specimen and the accompanying advance of the ice/water interface. Given that the water layer after wetting the contact
224   surfaces is very thin, the bond strength would be expected to saturate quickly; it is suggested that the process, similar
225   to above described phase (1), takes fewer than 30 minutes at -10 °C and a greater amount of time at -3 °C, aligning
226   with earlier studies and the result here. This means that for saline bonds, phase (3) has a duration of about 6…12
227   hours, whereas earlier experiments have occasionally had relatively long freezing times, varying from 60 h to 12 days
228   (Bailey et al., 2012; Shafrova and Høyland, 2008).

229

230   As part of the studies on the evolution of bond strength, it has been fairly common to investigate the ratio of
231   the bond strength values to that of the parent material (Bailey et al., 2012; Boroojerdi et al., 2020b; Shafrova and
232   Høyland, 2008). Shafrova and Høyland (2008) found that specimens with bonds grown in the field had the strength
233   ratio varying from 0.008 to 0.082 (with a mean of 0.03 after 48 hours of bonding). For laboratory-grown bonds, they
234   measured ratios in the range 0.06 to 0.69 (0.21 ± 0.12). The latter values are in line with values reported by Bailey et.
235   al. (2011) and Boroojerdi et al. (2020b), who reported ratios up to about 0.70 and 0.85, respectively. Boroojerdi et al.
236   (2020b) suggested an empirical formula to describe the strengthening of a freeze bond during the above-described
237   phase (3). The formula was based on curve fitting and an assumption that the shear strength of the bond approaches
238   asymptotically that of the parent material with increasing sintering time. The experiments here indicate that such an
239   assumption may not be always justified, as at least the flexural strength of the freeze bonds can reach values that are

240   above that of the parent material. Aligning with our observations, the results by Høyland and Møllegaard (2014)

241   provide an indication of the shear strength of freeze bonds reaching strengths comparable to that of the parent material.

242   In their uniaxial compression tests on bonded cylindrical samples having an inclined freeze-bond, the failure changed

243   from shearing (along the plane of the bond) to axial splitting of the sample in some of the cases.

244

245   Ettema and Schaefer (1986) and Repetto-Llamazares et al. (2011b) studied whether freezing in the presence

246   of water has an effect on the shear strength of the freeze-bond. The results indicate that shear strength was higher

247   when bonds froze under water. While Ettema and Schaefer (1986) let the bonding occur with samples submerged in

248   fresh water, Repetto-Llamazares et al. (2011b) used 7 ppt saline water for submerging. Earlier studies on the effect of

249   freezing conditions have not had the opposing surfaces wetted before bringing them together when generating bonds

250   in air. This effectively removes the above-described phase (1) from the bond strength evolution, if the result of the

251   heat transfer during the initial period of bond strengthening is assumed to simply be freezing of the liquid at the bond

252   interface. In addition, in these earlier studies, the maximum freezing times for the bonds grown in air varied only

253   from 0.5 min to 3 min. As phase (3) takes at least several hours, it seems likely that the mentioned studies have not

254   yielded data on saturated bond strengths for bonds grown in air.

255

256   While the new data from the present tests yielded clear trends for the strength of the freeze-bonds, they also

257   showed significant scatter. This scatter, even when bond generation was performed in a simplified manner using

258   carefully prepared milled samples (Section 2), is an indication that the strength of freeze bonds is a parameter that

259   inherently shows wide scatter. One reason for this, amongst others perhaps, is the detailed microstructure/phase

260   distribution of the bond. The microstructure probably varies somewhat from specimen to specimen, thereby leading

261   to variations in bond strength. The variation is actually of similar magnitude to that observed in experiments on the

262   flexural strength of pristine ice samples made with the same apparatus (Murdza et al., 2020c). The other reason,

263   perhaps, can be attributed to the fact that a small volume of material is tested in bending and, hence, the variation in

264   tensile strength if measured using a traditional methodology would likely be smaller, given the correlation coefficient

265   between tensile and flexural strength is 1.7.

266

267   The fact that in samples with freshwater bonds failure initiated and propagated outside of the bond suggests

268   that the strength of the freshwater bond is greater than the strength of pristine freshwater S2 ice. This may indicate a

269   difference in microstructure between the ice in the freeze bond and the ice of the parent plates. A finer grain size

270   within the bonds may be due to the initial water layer, which was produced by spraying a very fine mist, creating small

271   water droplets working as nucleation sites for the ice grains in the bond. Our argument is supported by the work of

272   Schulson and others (1984) who showed that tensile strength strongly depends on the grain size, increasing as grain

273   size decreases. A difference in grain size could also explain the fact that the strength versus salinity curve from Timco

274   and O'Brien (1994) is below the trend obtained in the present study (Figure 3). Concerning of the microstructure of

275   the bonds, one may think that because one phase is dominant it should form the matrix; however, there is at least one

276   class of materials, namely high-temperature nickel-based superalloys (Sims, 1984) where the minor component forms

277 the matrix. Since we do not know the structure of the bonds in the present study, we cannot be conclusive in this
278 regard.

279

280 As expected, both temperature and salinity affect the flexural strength of bonded ice samples. The strength
281 of both freshwater and saline ice increases over time and saturates, although saturation occurs significantly slower in
282 the case of saline bonds. The reason is likely related to the rejected salts and entrapped air at the ice-water inferface
283 that slows the rate of the interface advance. The trend of saturated strength versus salinity (Figure 3) has an exponential
284 functionality similar to what has been suggested by Timco and O'Brien (1994), while the trend of saturated strength
285 versus temperature for saline bonds (Figure 4) appears, to a first approximation, to be roughly linear. It is important
286 to mention here that the salinities provided in this paper are salinities of the spray and not of melt-water from the bond
287 itself, and this begs the question: Is the bond salinity the same or lower than the salinity of spray solution? In the
288 formation of a natural floating sea ice cover, of course, the rejection of salts from ice results in melt-water salinities
289 lower than bulk water salinity (Weeks and Ackley, 1986). Given that in our experiments the bond thickness is very
290 small (<1 mm) and freezing time is relatively short, it is unlikely that all the salt is expelled from the freeze bond,
291 resulting in the bond salinity similar to the spray salinity. Therefore, while the resulting bonds might have salinities
292 slightly lower than the sprayed water, the results yield a reasonably reliable trend of strength as a function of salinity
293 which is very similar to the relationship proposed by Timco and O'Brien (1994).

294

295 The effect of surface roughness at the freezing interface was also briefly addressed when performing the
296 experiments. In addition to the milled surfaces with a roughness of $0.43\pm0.24 \times 10^{-6}$ m in the direction of milling and
297 $2.01\pm0.47 \times 10^{-6}$ m in the orthogonal direction (Schulson and Fortt, 2012), experiments were performed on samples
298 with surfaces produced by using a fine and coarse band saw blade, which resulted in ice surface roughness of up to
299 ~1 mm. The results from the experiments with differently produced surfaces showed no significant difference on the
300 strength of freshwater and saline bonds (1.39 MPa vs 1.43 ± 0.15 MPa for freshwater bonds and 0.39 ± 0.13 MPa vs
301 0.34 ± 0.16 MPa for saline bonds of 12 ppt salinity). As milling could be performed with the highest accuracy from the
302 aspect of sample dimensions and alignment, it was chosen as the technique we used here. Unlike what was observed
303 in the present study, Helgøy et al. (2013a) observed that the surface roughness does affect freeze bond shear strengths,
304 with rougher surface leading to bonds having higher strength. The discrepancy between their results and results in the
305 present study suggests that there may exist a threshold value for the surface roughness, after which it affects the bond
306 strength; it is likely that both milled and sawn surfaces used in the present study are too smooth for the effect of surface
307 roughness to be observed. On the other hand, experiments on shear strength usually involve sliding motion between
308 the blocks of the parent material. This motion may become restricted by rough surfaces, which could lead to higher
309 shear loads interpreted to be due to an increase in freeze-bond strength. In tests under tensile loading, such kinematic
310 restrictions do not exist.

311

312   Finally, it is worth noting that while this is the first study on the flexural strength of freeze bonds, it is not

313   the complete story. Further work is needed to investigate the effects of other factors such as bond pressure, the

314   character of parent ice plate, bond microstructure, the width of the opening to be bonded, etc.

5. Conclusions

316   Systematic experiments on the flexural strength of freeze bonds were conducted for the first time. The bonds

317   were grown in the air under 4 kPa confining pressure. The parent material was S2 columnar-grained freshwater ice.

318   The salinity of the bond varied from 0 to 35 ppt and freezing temperatures from -3 to -25 °C. It is concluded that:

319   (i)   Freshwater bond strength exceeds the strength of parent ice in less than 0.5 h upon freezing.

320   (ii)   The saline bonds reach their saturated strength within about 6-12 h of freezing.

321   (iii)   An increase in bond salinity and in freezing temperature leads to a decrease in bond strength.

322   (iv)   The relationship between bond strength and its salinity is similar to the one suggested by Timco and O'Brien

323   (1994).

324   (v)   No freezing occurs once the salinity of the water used to generate the bond reaches values of about ~25 ppt

325   at -3 °C.

Acknowledgements

327   The authors are grateful for the financial support from the Academy of Finland through the project no. 309830 ("Ice

328   Block Breakage: Experiments and Simulations (ICEBES)") and National Science Foundation (FAIN 1947-107). Arttu

329   Polojärvi worked on the article while visiting Thayer School of Engineering at Dartmouth College (Hanover, NH,

330   USA) during spring 2020, thanks are extended to Prof. Erland Schulson for hosting. Finnish Maritime Foundation is

331   acknowledged for partial funding of the visit.

332

333   **Author contributions:** AM, AP, ES, and CR designed the experiments, and AM carried them out. AM and AP

334   prepared the manuscript with contributions from all co-authors.

335

336   **Competing interests:** The authors declare that they have no conflict of interest.

References

338   Ardhuin, F., Otero, M., Merrifield, S., Grouazel, A. and Terrill, E.: Ice Breakup Controls Dissipation of Wind Waves

339   Across Southern Ocean Sea Ice, Geophys. Res. Lett., 47(13), doi:10.1029/2020GL087699, 2020.

340   Ashby, M. M. and Jones, D. R. H.: Engineering Materials 1: An Introduction to Properties, Applications and Design,

341   4th ed., Elsevier/Butterworth-Heinemann, Oxford, UK., 2012.

342 Asplin, M. G., Galley, R., Barber, D. G. and Prinsenberg, S.: Fracture of summer perennial sea ice by ocean swell as
343 a result of Arctic storms, J. Geophys. Res. Ocean., 117(6), 1–12, doi:10.1029/2011JC007221, 2012.

344 Bailey, E., Sammonds, P. R. and Feltham, D. L.: The consolidation and bond strength of rafted sea ice, Cold Reg. Sci.
345 Technol., 83–84, 37–48, doi:10.1016/j.coldregions.2012.06.002, 2012.

346 Boroojerdi, M. T., Bailey, E. and Taylor, R.: Experimental investigation of rate dependency of freeze bond strength,
347 Cold Reg. Sci. Technol., 178, 1–12, doi:10.1016/j.coldregions.2020.103120, 2020a.

348 Boroojerdi, M. T., Bailey, E. and Taylor, R.: Experimental study of the effect of submersion time on the strength
349 development of freeze bonds, Cold Reg. Sci. Technol., 172, 1–16, doi:10.1016/j.coldregions.2019.102986, 2020b.

350 Bueide, I. M. and Høyland, K. V.: Confined compression tests on saline and fresh freeze-bonds, in Proceedings of the
351 23rd International Conference on Port and Ocean Engineering under Arctic Conditions, Trondheim, Norway., 2015.

352 Carter, D.: Lois et mechanisms de l'apparente fracture fragile de la glace de riviere et de lac, PhD Thesis, University
353 of Laval., 1971.

354 Collins, C. O., Rogers, W. E., Marchenko, A. and Babanin, A. V.: In situ measurements of an energetic wave event
355 in the Arctic marginal ice zone, Geophys. Res. Lett., 42(6), 1863–1870, doi:10.1002/2015GL063063, 2015.

356 Ettema, R. and Schaefer, J. A.: Experiments on Freeze-Bonding Between Ice Blocks in Floating Ice rubble, J. Glaciol.,
357 32(112), 397–403, doi:10.3189/S0022143000012107, 1986.

358 Ettema, R. and Urroz, G. E.: On internal friction and cohesion in unconsolidated ice rubble, Cold Reg. Sci. Technol.,
359 16(3), 237–247, doi:10.1016/0165-232X(89)90025-6, 1989.

360 Frankenstein, G. and Garner, R.: Equations for Determining the Brine Volume of Sea Ice from −0.5° to −22.9°C., J.
361 Glaciol., 6(48), 943–944, doi:10.3189/S0022143000020244, 1967.

362 Golding, N., Schulson, E. M. and Renshaw, C. E.: Shear faulting and localized heating in ice: The influence of
363 confinement, Acta Mater., 58, 5043–5056, doi:10.1016/j.actamat.2010.05.040, 2010.

364 Golding, N., Snyder, S. A., Schulson, E. M. and Renshaw, C. E.: Plastic faulting in saltwater ice, J. Glaciol., 60(221),
365 447–452, doi:10.3189/2014JoG13J178, 2014.

366 Heinonen, J.: Constitutive modeling of ice rubble in first-year ridge keel, Aalto University., 2004.

367 Helgøy, H., Astrup, O. S. and Høyland, K. V.: Laboratory work on freeze-bonds in ice rubble, Part I: Experimental
368 set-up, Ice-properties and freeze-bond texture, in Proceedings of the 22nd International Conference on Port and Ocean
369 Engineering under Arctic Conditions, Espoo, Finland., 2013a.

370 Helgøy, H., Astrup, O. S. and Høyland, K. V.: Laboratory work on freeze-bonds in ice rubble, Part II – Results from
371 individual freeze bond experiments, in Proceedings of the 22nd International Conference on Port and Ocean
372 Engineering under Arctic Conditions, Espoo, Finland., 2013b.

373 Høyland, K. V. and Møllegaard, A.: Mechanical behaviour of laboratory made freeze-bonds as a function of
374 submersion time, initial ice temperature and sample size, in 22nd IAHR International Symposium on Ice, pp. 265–
375 273, Singapore., 2014.

376 Hwang, B., Wilkinson, J., Maksym, E., Graber, H. C., Schweiger, A., Horvat, C., Perovich, D. K., Arntsen, A. E.,
377 Stanton, T. P., Ren, J. and Wadhams, P.: Winter-to-summer transition of Arctic sea ice breakup and floe size
378 distribution in the Beaufort Sea, Elem Sci Anth, 5, 40, doi:10.1525/elementa.232, 2017.

379   Iliescu, D., Murdza, A., Schulson, E. M. and Renshaw, C. E.: Strengthening ice through cyclic loading, J. Glaciol.,
380   63(240), 663–669, doi:10.1017/jog.2017.32, 2017.

381   Kohout, A. L., Williams, M. J. M., Dean, S. M. and Meylan, M. H.: Storm-induced sea-ice breakup and the
382   implications for ice extent, Nature, 509(7502), 604–607, doi:10.1038/nature13262, 2014.

383   Kohout, A. L., Williams, M. J. M., Toyota, T., Lieser, J. and Hutchings, J.: In situ observations of wave-induced sea
384   ice breakup, Deep. Res. Part II Top. Stud. Oceanogr., 131, 22–27, doi:10.1016/j.dsr2.2015.06.010, 2016.

385   Liferov, P., Jensen, A. and Høyland, K. V.: On analysis of punch tests on ice rubble, in Proceedings of the 16th
386   International Symposium on Ice, volume 2, pp. 101–110, Dunedin, New Zealand., 2002.

387   Liferov, P., Jensen, A. and Høyland, K. V.: 3D finite element analysis of laboratory punch tests on ice rubble, in
388   Proceedings of the 17th International Conference on Port and Ocean Engineering under Arctic Conditions, POAC'03,
389   volume 2, pp. 611–621, Trondheim, Norway., 2003.

390   Marchenko, A. and Chenot, C.: Regelation of ice blocks in the water and on the air, in Proceedings of the 20th
391   International Conference on Port and Ocean Engineering under Arctic Conditions, Luleå, Sweden., 2009.

392   Michel, B. and Ramseier, R. O.: Classification of river and lake ice, Can. Geotech. J., 8(1), 36–45, doi:10.1139/t71-
393   004, 1971.

394   Murdza, A., Schulson, E. M. and Renshaw, C. E.: Hysteretic behavior of freshwater ice under cyclic loading :
395   preliminary results, in 24th IAHR International Symposium on Ice, pp. 185–192, Vladivostok., 2018.

396   Murdza, A., Schulson, E. M. and Renshaw, C. E.: The effect of cyclic loading on the flexural strength of columnar
397   freshwater ice, in Proceedings of the International Conference on Port and Ocean Engineering under Arctic
398   Conditions, POAC, vol. 2019-June., 2019.

399   Murdza, A., Schulson, E. and Renshaw, C.: Behavior of Saline Ice under Cyclic Flexural Loading, Cryosph. Discuss.,
400   1–22, doi:10.5194/tc-2020-300, in press, 2020a.

401   Murdza, A., Marchenko, A., Schulson, E., Renshaw, C., Sakharov, A., Karulin, E. and Chistyakov, P.: Results of
402   preliminary cyclic loading experiments on natural lake ice and sea ice, in 25th IAHR International Symposium on Ice,
403   pp. 1–10, Trondheim, Norway., 2020b.

404   Murdza, A., Schulson, E. M. and Renshaw, C. E.: Strengthening of columnar-grained freshwater ice through cyclic
405   flexural loading, J. Glaciol., 66(258), 556–566, doi:10.1017/jog.2020.31, 2020c.

406   Murdza, A., Marchenko, A., Schulson, E. M. and Renshaw, C. E.: Cyclic strengthening of lake ice, J. Glaciol., 67(261),
407   182–185, doi:10.1017/jog.2020.86, 2021.

408   Polojärvi, A. and Tuhkuri, J.: On modeling cohesive ridge keel punch through tests with a combined finite-discrete
409   element method, Cold Reg. Sci. Technol., 85, 191–205, doi:10.1016/j.coldregions.2012.09.013, 2013.

410   Repetto-Llamazares, A. H. V., Høyland, K. V. and Kim, E.: Experimental studies on shear failure of freeze-bonds in
411   saline ice:. Part II: Ice-ice friction after failure and failure energy, Cold Reg. Sci. Technol., 65(3), 298–307,
412   doi:10.1016/j.coldregions.2010.12.002, 2011a.

413   Repetto-Llamazares, A. H. V., Høyland, K. V. and Evers, K. U.: Experimental studies on shear failure of freeze-bonds
414   in saline ice: Part I. Set-up, failure mode and freeze-bond strength, Cold Reg. Sci. Technol., 65(3), 286–297,
415   doi:10.1016/j.coldregions.2010.12.001, 2011b.

416 Schulson, E. M. and Fortt, A. L.: Friction of ice on ice, J. Geophys. Res. Solid Earth, 117(B12), n/a-n/a,
417 doi:10.1029/2012JB009219, 2012.

418 Schulson, E. M., Lim, P. N. and Lee, R. W.: A brittle to ductile transition in ice under tension, Philos. Mag. A, 49(3),
419 353–363, doi:10.1080/01418618408233279, 1984.

420 Serré, N.: Mechanical properties of model ice ridge keels, Cold Reg. Sci. Technol., 67(3), 89–106,
421 doi:10.1016/j.coldregions.2011.02.007, 2011a.

422 Serré, N.: Numerical modelling of ice ridge keel action on subsea structures, Cold Reg. Sci. Technol., 67(3), 107–119,
423 doi:10.1016/j.coldregions.2011.02.011, 2011b.

424 Serré, N., Repetto-Llamazares, A. H. V. and Høyland, K.: Experiments on the relation between freezebond and ice
425 rubble strength, part I: shear box experiments, in Proceedings of the 21st International Conference on Port and Ocean
426 Engineering under Arctic Conditions, pp. 1–18, Montreal, Canada., 2011.

427 Shackleton, E. H.: South: The Story of Shackleton's Last Expedition, 1914–17, Macmillian, USA., 1982.

428 Shafrova, S. and Høyland, K. V.: The freeze-bond strength in first-year ice ridges. Small-scale field and laboratory
429 experiments, Cold Reg. Sci. Technol., 54(1), 54–71, doi:10.1016/j.coldregions.2007.11.005, 2008.

430 Shen, H. H.: Wave-Ice Interactions, in Encyclopedia of Maritime and Offshore Engineering, John Wiley & Sons, Ltd,
431 Chichester, UK., 2017.

432 Sims, C. T.: A History of Superalloy Metallurgy for Superalloy Metallurgists, in Superalloys 1984 (Fifth International
433 Symposium), pp. 399–419, The Minerals, Metals and Materials Society, Warrendale, PA., 1984.

434 Smith, T. R. and Schulson, E. M.: The brittle compressive failure of fresh-water columnar ice under biaxial loading,
435 Acta Metall. Mater., 41(1), 153–163, doi:10.1016/0956-7151(93)90347-U, 1993.

436 Snyder, S. A., Schulson, E. M. and Renshaw, C. E.: Effects of prestrain on the ductile-to-brittle transition of ice, Acta
437 Mater., 108, 110–127, doi:10.1016/j.actamat.2016.01.062, 2016.

438 Squire, V. A.: Ocean Wave Interactions with Sea Ice: A Reappraisal, Annu. Rev. Fluid Mech., 52(1), 37–60,
439 doi:10.1146/annurev-fluid-010719-060301, 2020.

440 Szabo, D. and Schneebeli, M.: Subsecond sintering of ice, Appl. Phys. Lett., 90(151916), 1–3, doi:10.1063/1.2721391,
441 2007.

442 Timco, G. W. and O'Brien, S.: Flexural strength equation for sea ice, Cold Reg. Sci. Technol., 22(3), 285–298,
443 doi:10.1016/0165-232X(94)90006-X, 1994.

444 Timco, G. W. and Weeks, W. F.: A review of the engineering properties of sea ice, Cold Reg. Sci. Technol., 60(2),
445 107–129, doi:10.1016/J.COLDREGIONS.2009.10.003, 2010.

446 Weeks, W. F. and Ackley, S. F.: The Growth, Structure, and Properties of Sea Ice, in The Geophysics of Sea Ice, pp.
447 9–164, Springer US, Boston, MA., 1986.

448

449

450

451

452 **Appendix A: The strength of freeze-bonds as a function of salinity and temperature**

453 Principle:

454

455   The freeze bond is comprised of essentially two phases, solid (ice) plus liquid (water), barring entrapped air.

456 To a first approximation, we assume that its strength, σ_{fb}, is proportional to the volume fraction, f_s, of the solid phase.

457 The constant of proportionality, σ_{f0}, is the strength of freshwater ice. The relationship:

$$\sigma_{fb} = \sigma_{f0} f_s \ . \tag{A3}$$

458 The volume fraction of the solid phase is obtained from the lever rule:

$$f_s = \frac{X_l - X_0}{X_l - X_s} \ , \tag{A4}$$

459 where X_l and X_s denote the limit of solubility of salt in the liquid (water) and in the solid (ice) phases, respectively,

460 and X_0 is the concentration of salt in the water before freezing is initiated. Over the temperature range of interest, the

461 phase diagram for the H_2O-NaCl system (i.e., thermodynamics) dictates that both X_l and X_s increases with decreasing

462 temperature, T, according to the relationships:

$$X_l = \frac{T - T_0}{m_l} \ , \tag{A5}$$

$$X_s = \frac{T - T_0}{m_s} \ , \tag{A6}$$

463 where T_0 denotes the melting point of "pure" ice (273 K) and m_l and m_s, respectively, denote the slope of the liquidus

464 and the solidus on the phase diagram; both slopes are negative. The solubility of salt in ice is very low and so for

465 practical purposes $X_s \sim 0$. Writing the temperature difference as $T - T_0 = \Delta T$, the volume fraction of ice within the

466 freeze bond from Eqn (A4) is given by:

$$f_s = \left(1 - \frac{m_l X_0}{\Delta T}\right) \ . \tag{A7}$$

467 Thus, upon equating X_0 to salinity, S, the strength of the freeze bond is given by:

$$\sigma_{fb} = \sigma_{f0} \left(1 - \frac{m_l S}{\Delta T}\right) \ . \tag{A8}$$

468 Taking m_l to be independent of concentration, its value is $m_l = -0.1 \ Kpsu^{-1}$, giving:

$$\sigma_{fb} = \sigma_{f0} \left(1 + \frac{0.1S}{\Delta T}\right) \ , \tag{A9}$$

469 where $\Delta T < 0$.

470

471 The model thus dictates that once freezing is complete the strength of the freeze bond decreases linearly with

472 increasing salinity, reaching the limit of zero strength when $S = \Delta T / -m_l$.

473

474   Both dictates are in reasonable agreement with observation.

475

476   **Appendix B: Trends in Figure 3**

477

478   The red trend in Figure 3 is taken from (Timco and O'Brien, 1994) where the authors report values for

479   flexural strength of saline ice over the range of salinities used in the present study and for temperatures above -4.5°C

480   (σ_f in MPa), i.e.

481

$$\sigma_f = 1.76e^{-5.88\sqrt{v_b}}. \tag{A10}$$

482

483

484   To calculate salinity S (in ppt) based on the liquid brine content v_b (brine volume fraction) in Timco and

485   O'Brien (1994) we used the following relationship suggested by (Frankenstein and Garner, 1967):

486

$$v_b = S\left(\frac{49.185}{|T|} + 0.532\right) \tag{A11}$$

487

488   where T is the ice temperature in degrees Celsius between -0.5 °C and -22.9 °C. The fit to our data in Figure 3 (black

489   curve) was made according to the least square method which resulted in the following equation (σ_f in MPa):

490

$$\sigma_f = 1.12e^{-5.88v_b} \tag{A12}$$

491

492

493

494

495

496

497

498

499

500

501

502

503

504

505

506

507

508

509

510

511

512

513

514 **Table 1. Results from testing freshwater bond experiments. The time here is the bond formation time, the strength is the**

515 **flexural strength (temperature during flexural testing and bond formation was the same). The reader should notice that in**

516 **all of these experiments the failure occurred outside of the bond and within the parent material.**

Sample #	Temperature [°C]	Time [h]	Strength [MPa]
1	-10	24	1.43
2	-10	25	1.39
3	-10	24	1.28
4	-10	3	1.58
5	-3	1.5	1.02
6	-3	1.5	1.28
7	-3	0.5	1.4

517

518 **Table 2. Results from testing saline bond experiments at -10 °C and 35 ppt.**

Sample #	Time [h]	Strength [MPa]
8	1.5	0.15
9	3	0.1
10	26	0.34
11	34	0.54
12	25	0.64
13	82	0.61
14	6	0.38
15	12	0.54

519

520 **Table 3. Results from testing saline bond experiments at -3 °C and 12 ppt.**

Sample #	Time [h]	Strength [MPa]
16	1.5	Low
17	1.5	0.31
18	3	0.17
19	3	0.18
20	6	0.25
21	6	0.22
22	14	0.48
23	24	0.14

Sample #	Time [h]	Strength [MPa]
24	24	0.35
25	72	0.29
26	97	0.32

521

522

Table 4. Results from testing saline bond experiments at -3 °C.

Sample #	Salinity [ppt]	Time [h]	Strength [MPa]
27	35	1.5	No*
28	35	24	No*
29	25	24	No*
30	20	28	0.12
31	17	3	Low*
32	17	13	Low*
33	17	25	0.3
34	17	113	0.28
35	10	24	0.34
36	10	24	0.34
37	10	24	0.41
38	10	26	0.77
39	10	73	0.54
40	5	21	0.37
41	5	24	0.46
42	5	24	0.75
43	2	25	0.62
44	2	24	0.91

524 * "No" and "Low" correspond to "No freezing occurred" and "Strength was too small to be measured", respectively.

525

Table 5. Results from testing of ice with bond salinity of 20 ppt after ~24 h of freezing.

Sample #	Temperature [°C]	Strength [MPa]
45	-25	1.69*
46	-25	1.67*
47	-25	1.47*
48	-25	1.13
49	-20	1.25
50	-20	0.71
51	-15	0.87
52	-15	0.76
53	-15	0.63
54	-15	0.55

Sample #	Temperature [°C]	Strength [MPa]
55	-15	0.35
56	-15	0.2
57	-10	0.66
58	-10	0.64
59	-10	0.46
60	-10	0.4
61	-5	0.2
62	-5	0.1
63	-3	0.12

527 *failure occurred outside the bond.

528

529

530

531
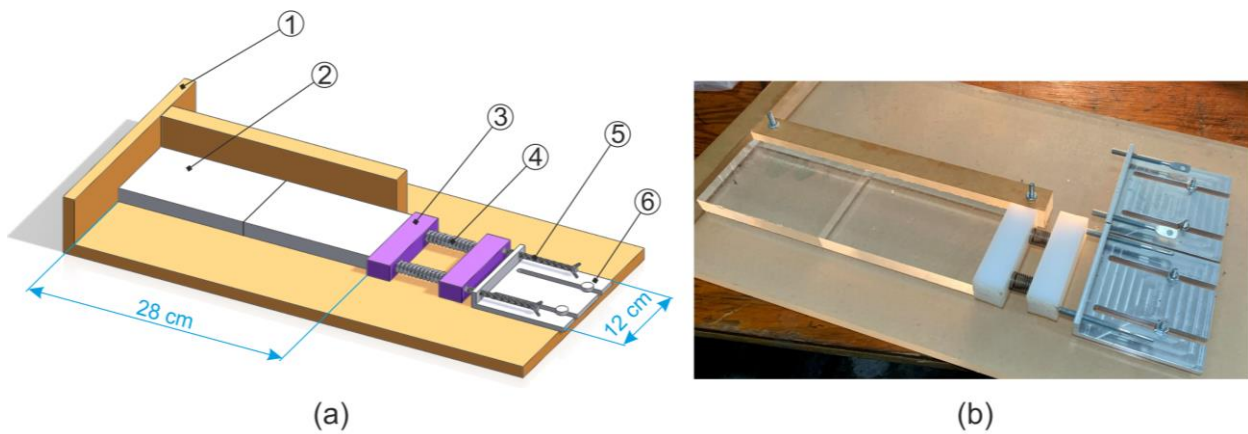
532 **Figure 1. Sketch (a) and photograph (b) of the freeze-bonding rig with an ice sample having the shape of a thin plate: 1 –**

533 **acrylic plate; 2 – ice specimen; 3 – plastic bar; 4 – spring; 5 – bolt; 6 – fixation plate.**

534
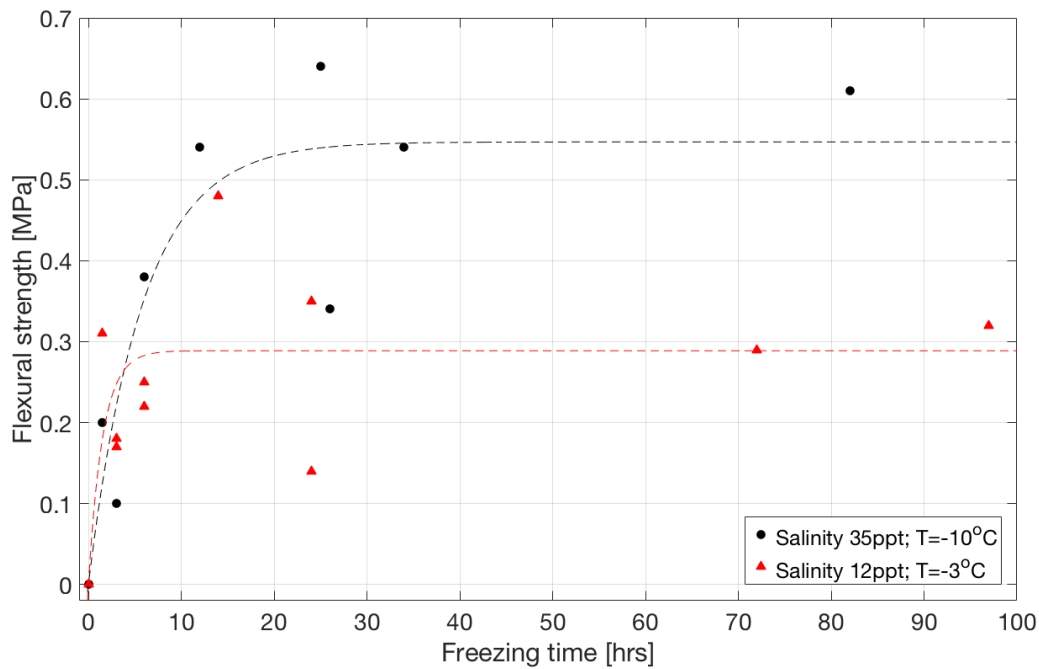
Figure 2. Flexural strength as a function of freezing time for bonded ice prepared from salt water of 35 ppt salinity at -10°C

536 **(in black) and from salt water of 12 ppt salinity at -3°C (in red).**
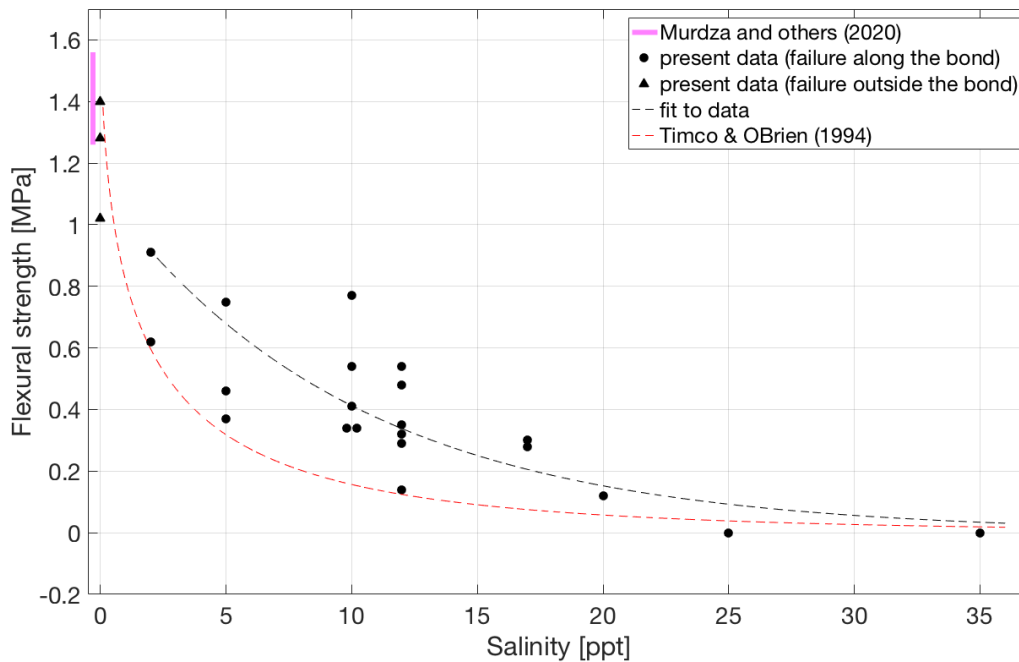
537

538 **Figure 3. Flexural strength at -3 °C of bonded ice as a function of the salinity of the salt water from which the bond was**

539 **formed. The solid pink line indicates the flexural strength 1.42±0.16 MPa of parent freshwater ice at -3 °C (Murdza et al.,**

540 **2020c). A red dashed line is taken from Timco and O'Brien (1994) for the ice at -3 °C. A black dashed line is a fit to the**

541 **present data.**

542
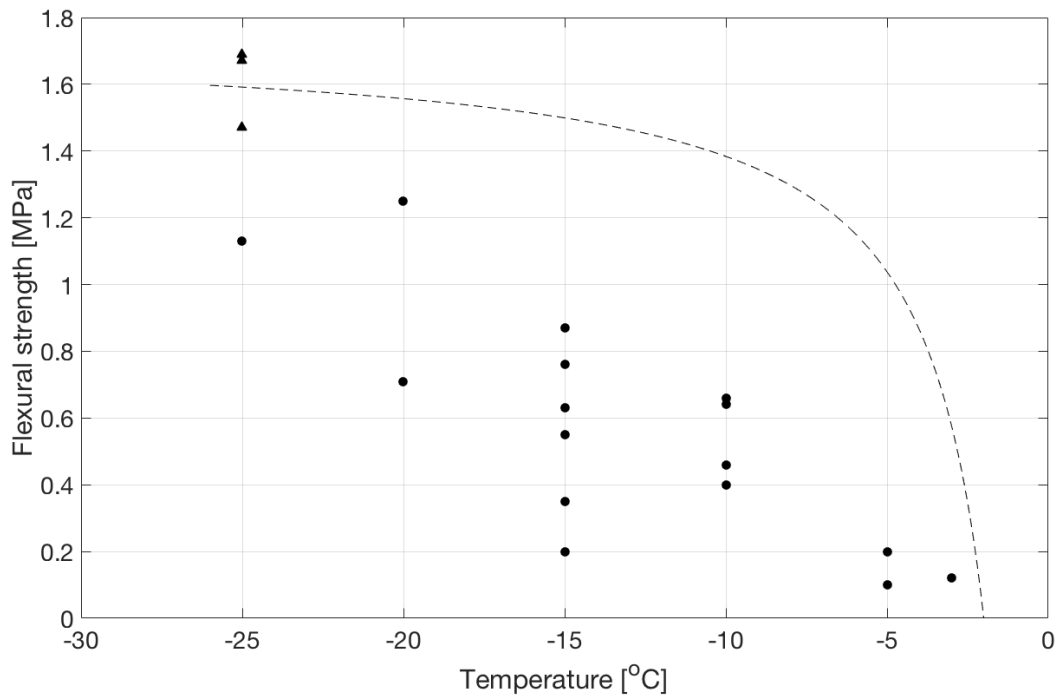
Figure 4. Flexural strength of bonded ice as a function of temperature for bonds formed from water of salinity of 20 ppt.

Triangular-shaped points at -25 °C indicate that actual bond strength is greater than that of the parent material as the

failure occurred outside the bond. The dotted line is drawn according to the model in Appendix A.

546
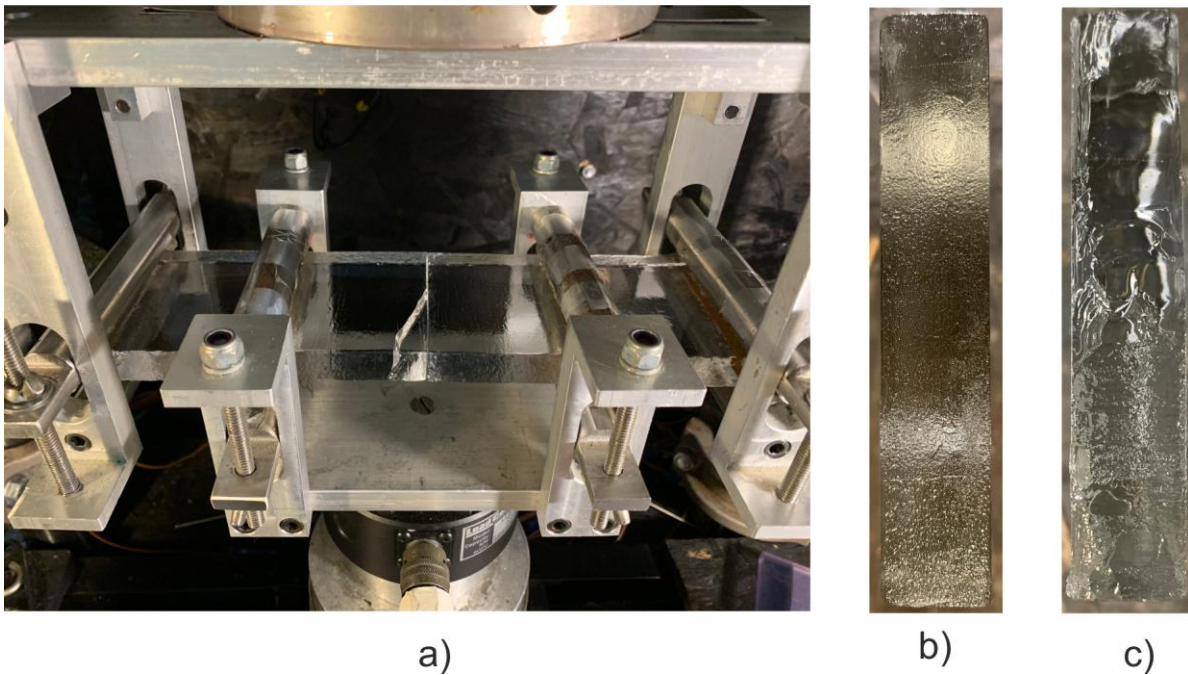
Figure 5. Photographs of an ice sample #38 right after forced failure (a); the saline bond surface of 10 ppt after a crack

propagated fully through the bond, sample #19 (b) and partially through the parent material, sample #47 (c).

549